

EFFECTS OF VARIABLE VISCOSITY AND THERMAL CONDUCTIVITY ON STEADY NATURAL CONVECTION COUETTE FLOW HAVING SUCTION/INJECTION

Tafida M. Kabir¹, Abiodun O. Ajibade² and Lawal Umar³

^{1,3}Department of Mathematics, Federal College of Education, Zaria, Nigeria.

²Department of Mathematics, Ahmadu Bello University, Zaria, Nigeria.

Abstract

This study examines the effect of variable viscosity and thermal conductivity on steady natural convection Couette flow having suction/injection. The governing Equations of momentum and energy are obtained and solved using the homotopy perturbation method. The effects of various parameters on the fluid velocity and temperature are depicted graphically and analysed in details. During the course of computation, it is found that an increasing viscosity corresponds to the increasing resistance to flow which suppress the velocity of the working fluid, decreasing the viscosity contributes a decrease in the temperature of the working fluid. It is further discovered that the thermal boundary layer thickness is also increased due to the corresponding strengthening of the convection currents caused by increase in the thermal conductivity and fluid velocity increases. Finally, to validate our results with the results of Jha and Ajibade (2010), an excellent agreement is found when the viscous dissipation, variable viscosity, variable thermal conductivity and suction/injection terms are neglected.

Keywords: natural convection; thermal conductivity; variable viscosity; suction/injection; Couette flow; Homotopy perturbation method.

1 Introduction

The fluid flows and heat transfer between vertical channels have considerable impact in the practical applications in various fields such as Thermal insulation, Geothermal Engineering, Petroleum manufactures, Solid matrix heat exchangers, Chemical catalytic reactors, groundwater hydrology, cooling of electronic systems and many others. Also, the study of boundary layer flow and suction or injection play an important role in many natural phenomena such as Engineering and Space Sciences. Pop and Watanabe [1] investigated the effects of suction or injection in boundary layer flow and heat transfer on a continuous moving surface. They discovered that the suction or injection has a profound effect on the boundary layer thickness. In general, injection prompts s-shaped velocity profiles and may exhibit overshoots in the thin slot. However, the net effect of suction is to reduce the overshooting tendency and slow down the flow. Shojaefard et al. [2] studied flow control on a Sabsonic airfoil by suction and injection. They reported that suction increases the lift coefficient while injection decreases the skin friction, which is transitively resulted in a considerable reduction in an energy consumed during flights of subsonic aircraft. Anuar et al. [3] studied uniform suction/blowing effect on flow and heat transfer due to stretching cylinder. They discovered that injection is a sufficient condition to reduce the skin friction. Hazeem [4] analyzed the effect of suction and injection on unsteady Couette flow with variable properties. He concluded that increasing the viscosity exponent increases the velocity and temperature for all values of the suction parameter and also increasing suction decreases velocity and temperature for all values of viscosity. Jha and Ajibade [5] investigated unsteady free convective Couette flow of heat generating/absorbing fluid. They discovered that an increase in heat absorption increases the rate of heat transfer on the moving plate and decreases the rate of heat transfer on the stationary plate. Jha et al. [6] analysed the entropy generation under the effect of suction/injection. Their outcomes show that entropy generation number increases with suction on one porous plate, while it decreases on the other porous plate with injection. Bala and Naikoti [7] studied viscous dissipation effects on unsteady free convection and mass transfer flow past an accelerated vertical porous plate with suction. They reported that the greater suction leads to reduction in the velocity, temperature and concentration distribution of the flow fields. Hazarika and Uptal [8] studied effects of variable viscosity and thermal conductivity on

Correspondence Author: Tafida M.K., Email: mktafida.555@gmail.com, Tel: +2348065539821, +2348067499557

Transactions of the Nigerian Association of Mathematical Physics Volume 15, (April - June, 2021), 139 –150

magnetohydrodynamics flow past a vertical channel. They observed that the velocity profile increases with the decreases of thermal conductivity. Daniel et al. [9] studied unsteady forced and free convection flow past an infinite permeable vertical plate. They discovered that the boundary layers increased towards the plate with injection and reduced towards the plate with suction. It is also seen that the temperature is higher near the plate with injection, while velocity is enhanced near the plate with suction and injection. Jha et al. [10] studied natural convection flow in a vertical micro-channel with suction/injection. They concluded that suction/injection on the micro-channel surfaces increases the volume flow rate due to a decrease in both velocity and temperature within the channel. Borah and Hazarika [11] presented effects of variable viscosity and thermal conductivity and magnetic field effect on the free convection and mass transfer flow through porous medium with constant suction/heat flux. They observed that temperature decreases for increase of both viscosity and thermal conductivity parameter. Oahimire and Olajuwon [12] considered hydromagnetic flow near a stagnation point on a stretching sheet with variable thermal conductivity and heat generation. They concluded that the temperature profile increases due to increase in thermal conductivity parameter. Uwanta and Hamza [13] examined the effect of suction/injection on unsteady hydromagnetic convective flow of reactive viscous fluid between vertical porous plates with thermal diffusion. They observed that temperature decreases due to suction but increases due to injection. In case of suction, the fluid at ambient conditions is brought closer to the surface and reduces the thermal boundary layer thickness. Jha et al. [14] investigated the role of suction/injection on magnetohydrodynamics natural convection flow in a vertical micro-channel. They reported that as suction on the hot porous wall with simultaneous injection on the cold porous wall increases, velocity decreases. In another article, Jha et al. [15] studied the effects of suction/injection-combination (SIC) on transient free convective-radiation flow in a vertical porous channel. They discovered that the introduction of suction/injection has distorted the symmetric nature of the flow. Santana and Hazarika [16] analysed the effects of variable viscosity and thermal conductivity on magnetohydrodynamics free convection and mass transfer flow over an inclined vertical surface in a porous medium with heat generation. They discovered that an increasing value of viscosity retard the velocity but enhance the temperature. Omokhuale and Ovwaso [17] considered the effect of heat source on free convection fluid flow in a vertical channel with chemical reaction. They concluded that the effect of suction/injection on velocity increases with the increase of injection for cooling of the channel and decreases the heating of the channel, and also clear that suction stabilizes the boundary layer. Hazarika and Phukan [18] investigated the effects of variable viscosity and thermal conductivity on steady magnetohydrodynamics flow of a micropolar fluid through a specially characterized horizontal channel. They concluded that the skin friction decreases and Nusselt numbers increases when viscosity increases. Tafida and Ajibade [19] studied the effect of variable viscosity on natural convection flow between vertical parallel plates in the presence of heat generation/absorption. They reported that the skin friction on both plates increase as viscosity increases. Ajibade and Tafida [20] considered the combined effect of variable viscosity and variable thermal conductivity on natural convection Couette flow. They reported that an increase in viscosity exhibit a retarding effect on the thermodynamics within the channel thereby causing a decrease in fluid velocity.

The objective of the present study is to investigate the effect of variable viscosity and thermal conductivity on steady natural convection Couette flow having suction/injection. The equations governing the flow are nonlinear and coupled so that obtaining closed form solution is a daunting task. Such problems can therefore be approached by numerical schemes or some approximate solution methods. One of the efficient methods is the perturbation method. However, solutions obtained by perturbation method are restricted to small perturbation parameters; therefore to overwhelm this restriction, alternative method called Homotopy perturbation method was presented. The convergence of the Homotopy perturbation method is so rapid that just a few terms of the series solution is required to achieve a high accuracy of the solutions. Due to the nonlinearity and coupling of the governing equations in the present situation, the method of Homotopy perturbation shall be employed to obtain the solutions of the momentum and energy equation. The obvious advantage of the Homotopy perturbation method in this work is that it can be applied to various nonlinear problems. The reliability of the method and the reduction in the size of the computational domain gives this method a wider applicability. Also, Homotopy perturbation method is very efficient and powerful tool to get the exact solution over other approximate analytical methods such as Differential transform method DTM, Adomian decomposition method ADM and Homotopy analysis method HAM. Homotopy perturbation method was introduced by He [21] to solve linear, nonlinear, and coupled problems in partial or ordinary form. Da-Hua [22] studied Homotopy perturbation method for nonlinear oscillators. From the computational point of view it is identified and proved beyond all doubts that the Homotopy perturbation method is very efficient and powerful tool for solving coupled and nonlinear system of differential equations. Abou-Zeid [23] investigated Homotopy perturbation method for magnetohydrodynamics non-Newtonian nanofluid flow through a porous medium in eccentric annuli with peristalsis. Sara and Bhatti [24] used Homotopy perturbation scheme to investigate the impact of impinging TiO₂ nanoparticles in Prandtl nanofluid along with endoscopic and variable magnetic field effects on peristaltic blood flow. In this paper, we extend the work of Jha and Ajibade [5] to investigate the effect of variable viscosity and thermal conductivity

on steady natural convection Couette flow in the presence of suction/injection. The fluid velocity and temperature are obtained and discussed for some carefully selected values of the flow parameters.

2 Mathematical Formulation of the Problem

The present problem considers natural convection Couette flow of viscous incompressible fluid in a vertical channel formed by two infinite parallel porous plates. The x^* -axis is taken vertically parallel to one of the porous plates of the channel and normal to the y^* -axis. The porous plates are stationary and parallel to each other at distance apart as shown in Figure 1. The plate at $y=0$ moves impulsively in its own plane with uniform velocity U while the other plate, which is placed h distance away from the first one remain stationary. The second plate is placed h distance away from the first. The temperature of the fluid and one of the channel plates are kept at T_0 while the temperature of the plate $y=0$ is raised or fell to T_w and thereafter maintained constant. Also, the plate $y=0$ moves in its own plane impulsively with a uniform velocity $u=U$ while the other plate remains at rest.

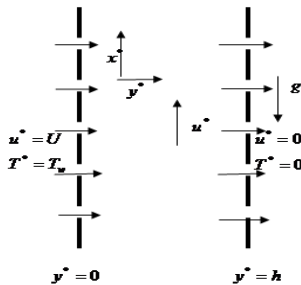


Figure 1: Schematic diagram of the problem

Under the usual assumption of Boussinesq's approximation, the governing dimensional equations of the energy and momentum are:

$$\frac{1}{\rho} \frac{d}{dy^*} \left(\mu^* \frac{du^*}{dy^*} \right) - q^* \frac{dT^*}{dy^*} + g\beta(T^* - T_0) = 0 \quad (1)$$

$$\frac{1}{\rho c_p} \frac{d}{dy^*} \left(k^* \frac{dT^*}{dy^*} \right) - q^* \frac{dT^*}{dy^*} - \frac{Q_0}{\rho c_p} (T^* - T_0) + \frac{\mu^*}{\rho c_p} \left(\frac{du^*}{dy^*} \right)^2 = 0 \quad (2)$$

Here u^* is the dimensional velocity, T^* is the dimensional temperature. y^* is the dimensional distance. β is the coefficient of thermal expansion, ρ is the density of the fluid, c_p is the specific heat constant pressure, Q_0 is the heat generation/absorption coefficient, k^* is the thermal conductivity, q^* is the suction/injection coefficient and g is the acceleration due to gravity.

While the boundary conditions that satisfy the problem are:

$$\begin{aligned} u^* &= U, T^* = T_w \text{ at } y^* = 0, \\ u^* &= 0, T^* = T_0 \text{ at } y^* = h. \end{aligned} \quad (3)$$

where U is the velocity of the moving plate, T_w is the temperature of the heated plate and T_0 temperature of the cold plate respectively. By introducing the following dimensionless quantities:

$$\begin{aligned} y &= \frac{y^*}{h}, u = \frac{u^*}{U}, T = \frac{T^* - T_0}{T_w - T_0}, Ec = \frac{U^2}{c_p (T_w - T_0)}, Pr = \frac{\mu c_p}{k}, Gr = \frac{g\beta h^3 (\theta_w - \theta_0)}{\nu U} \\ S &= \frac{Q_0 h^2}{k}, \mu^* = \mu_0 (1 - \lambda(T^* - T_0)), k^* = k_0 (1 - \varepsilon(T^* - T_0)), q = \frac{q^* h}{\nu_0} \end{aligned} \quad (4)$$

Where u is the dimensionless velocity, T is the dimensionless temperature, y is the dimensionless coordinate normal to the channel walls, Pr is the Prandtl number, S is the heat generation/absorption, μ the viscosity coefficient, k is the thermal conductivity, Ec is the viscous dissipation and q is the suction/injection.

Applying the usual Boussinesq approximation to equations (1) and (2), the momentum and energy equations in the dimensionless form are

$$(1-\lambda T) \frac{d^2 u}{dy^2} - q \frac{du}{dy} - \lambda \frac{du}{dy} \cdot \frac{dT}{dy} + Gr(1-\lambda T)T = 0 \quad (5)$$

$$(1-\lambda T)(1-\varepsilon T) \frac{d^2 T}{dy^2} - \varepsilon(1-\lambda T) \left(\frac{dT}{dy} \right)^2 - qPr(1-\varepsilon T) \frac{dT}{dy} - S(1-\lambda T)(1-\varepsilon T)T + EcPr(1-\varepsilon T) \left(\frac{du}{dy} \right)^2 = 0 \quad (6)$$

The boundary conditions in the dimensionless form for the physical system considered in the present work are:

$$\begin{aligned} u = 1, T = 1, \text{ at } y = 0, \\ u = 0, T = 0, \text{ at } y = 1. \end{aligned} \quad (7)$$

2.1 Solution by Homotopy Perturbation Method

Apply the Homotopy perturbation technique to solve the governing equations in the present problem, we construct a convex Homotopy on equations (5) and (6) to get

$$H(u, p) = (1-p) \left(\frac{d^2 u}{dy^2} \right) + p \left(\frac{d^2 u}{dy^2} - \lambda T \frac{d^2 u}{dy^2} - q \frac{du}{dy} - \lambda \frac{du}{dy} \cdot \frac{dT}{dy} + GrT - \lambda GrT^2 \right) = 0, \quad (8)$$

$$\begin{aligned} H(T, p) = (1-p) \left(\frac{d^2 T}{dy^2} \right) + p \left(\frac{d^2 T}{dy^2} - \lambda T \frac{d^2 T}{dy^2} - \varepsilon T \frac{d^2 T}{dy^2} + \lambda \varepsilon T^2 \frac{d^2 T}{dy^2} + \varepsilon \left(\frac{dT}{dy} \right)^2 \right) \\ - \lambda \varepsilon T \left(\frac{dT}{dy} \right)^2 - qPr \frac{dT}{dy} + \varepsilon qPrT - ST + \varepsilon ST^2 - \lambda \varepsilon ST^3 + EcPr \left(\frac{du}{dy} \right)^2 \\ - \varepsilon EcPrT \left(\frac{du}{dy} \right)^2 = 0, \end{aligned} \quad (9)$$

Simplify

$$\frac{d^2 u}{dy^2} - \lambda T \frac{d^2 u}{dy^2} - q \frac{du}{dy} - \lambda \frac{du}{dy} \cdot \frac{dT}{dy} + GrT - \lambda GrT^2 = 0, \quad (10)$$

$$\begin{aligned} \frac{d^2 T}{dy^2} - \lambda T \frac{d^2 T}{dy^2} - \varepsilon T \frac{d^2 T}{dy^2} + \lambda \varepsilon T^2 \frac{d^2 T}{dy^2} + \varepsilon \left(\frac{dT}{dy} \right)^2 - \lambda \varepsilon T \left(\frac{dT}{dy} \right)^2 - qPr \frac{dT}{dy} \\ + \varepsilon qPrT - ST + \varepsilon ST^2 + \lambda ST^2 - \lambda \varepsilon ST^3 + EcPr \left(\frac{du}{dy} \right)^2 - \varepsilon EcPrT \left(\frac{du}{dy} \right)^2 = 0. \end{aligned} \quad (11)$$

Using infinite series (5) and (6) to define u and T as follows

$$\begin{aligned} u = u_0 + pu_1 + p^2 u_2 + \dots, \\ T = T_0 + pT_1 + p^2 T_2 + \dots, \end{aligned} \quad (12)$$

Substituting (12) into (10) and (11) and simplifying, we have the following

$$\begin{aligned} \frac{d^2 u_0}{dy^2} + p \frac{d^2 u_1}{dy^2} + p^2 \frac{d^2 u_2}{dy^2} + \dots = p \lambda T_0 \frac{d^2 u_0}{dy^2} + p^2 \left(\lambda T_0 \frac{d^2 u_1}{dy^2} + \lambda T_1 \frac{d^2 u_0}{dy^2} \right) + \dots \\ + pq \frac{du_0}{dy} + p^2 q \frac{du_1}{dy} + \dots + p \lambda \frac{du_0}{dy} \cdot \frac{dT_0}{dy} \\ + p \left(\frac{du_0}{dy} \cdot \frac{dT_1}{dy} + \lambda \frac{du_1}{dy} \cdot \frac{dT_0}{dy} \right) + \dots - pGrT_0 \\ - p^2 GrT_1 - \dots + p \lambda GrT_0^2 + p^2 (2\lambda GrT_0 T_1) + \dots \end{aligned} \quad (13)$$

Similarly,

$$\begin{aligned} \frac{d^2 T_0}{dy^2} + p \frac{d^2 T_1}{dy^2} + p^2 \frac{d^2 T_2}{dy^2} + \dots = p \varepsilon T_0 \frac{d^2 T_0}{dy^2} + p^2 \left(\varepsilon T_0 \frac{d^2 T_1}{dy^2} + \varepsilon T_1 \frac{d^2 T_0}{dy^2} \right) + \dots \\ + p \lambda T_0 \frac{d^2 T_0}{dy^2} + p^2 \left(\lambda T_0 \frac{d^2 T_1}{dy^2} + \lambda T_1 \frac{d^2 T_0}{dy^2} \right) + \dots \\ - p \lambda \varepsilon T_0^2 \frac{d^2 T_0}{dy^2} - p^2 \left(\lambda \varepsilon T_0^2 \frac{d^2 T_1}{dy^2} + 2\lambda \varepsilon T_0 T_1 \frac{d^2 T_0}{dy^2} \right) - \dots \end{aligned}$$

$$\begin{aligned}
 &+ p\varepsilon\left(\frac{dT_0}{dy}\right)^2 + p^2\left(2\varepsilon\frac{dT_0}{dy}\cdot\frac{dT_1}{dy}\right) + \dots - p\lambda\varepsilon T_0\left(\frac{dT_0}{dy}\right)^2 \\
 &- p^2\left(2\lambda\varepsilon T_0\frac{dT_0}{dy}\cdot\frac{dT_1}{dy}\right) - \dots + pq\Pr\frac{dT_0}{dy} + p^2q\Pr\frac{dT_1}{dy} + \dots \\
 &- p\varepsilon q\Pr T_0\frac{dT_0}{dy} - p^2\left(\varepsilon q\Pr T_0\frac{dT_1}{dy} + \varepsilon q\Pr T_1\frac{dT_0}{dy}\right) - \dots \\
 &+ pST_0 + p^2ST_1 + \dots - p\varepsilon ST_0^2 - p^2(2\varepsilon ST_0T_1) - \dots \\
 &- p\lambda\varepsilon ST_0^2 - p^2(2\lambda\varepsilon ST_0T_1) - \dots + p\lambda\varepsilon ST_0^3 + p^2(3\lambda\varepsilon ST_0^2T_1) + \dots \\
 &- pEc\Pr\left(\frac{du_0}{dy}\right)^2 - p^2\left(2Ec\Pr\frac{du_0}{dy}\cdot\frac{du_1}{dy}\right) - \dots \\
 &+ p\lambda Ec\Pr T_0\left(\frac{du_0}{dy}\right)^2 + p^2\left(2\lambda Ec\Pr T_0\frac{du_0}{dy}\cdot\frac{du_1}{dy}\right) + \dots \\
 &+ p\varepsilon Ec\Pr T_0\left(\frac{du_0}{dy}\right)^2 + p^2\left(2\varepsilon Ec\Pr T_0\frac{du_0}{dy}\cdot\frac{du_1}{dy}\right) + \dots \\
 &- p\lambda\varepsilon Ec\Pr T_0^2\left(\frac{du_0}{dy}\right)^2 \\
 &- p^2\left(2\lambda\varepsilon Ec\Pr T_0^2\frac{du_0}{dy}\cdot\frac{du_1}{dy} + 2\lambda\varepsilon Ec\Pr T_0T_1\left(\frac{du_0}{dy}\right)^2\right) - \dots
 \end{aligned} \tag{14}$$

By comparing the coefficient p^0 , p^1 and p^2 of equation (13) and (14), we have

$$p^0 : \frac{d^2u_0}{dy^2} = 0, \tag{15}$$

$$p^0 : \frac{d^2T_0}{dy^2} = 0, \tag{16}$$

$$p^1 : \frac{d^2u_1}{dy^2} = \lambda T_0\frac{d^2u_0}{dy^2} + q\frac{du_0}{dy} + \lambda\frac{du_0}{dy}\cdot\frac{dT_0}{dy} - GrT_0 + \lambda GrT_0^2, \tag{17}$$

$$\begin{aligned}
 p^1 : \frac{d^2T_1}{dy^2} &= \varepsilon T_0\frac{d^2T_0}{dy^2} + \lambda T_0\frac{d^2T_0}{dy^2} - \lambda\varepsilon T_0^2\frac{d^2T_0}{dy^2} + \varepsilon\left(\frac{dT_0}{dy}\right)^2 - \lambda\varepsilon T_0\left(\frac{dT_0}{dy}\right)^2 \\
 &+ q\Pr\frac{dT_0}{dy} - \varepsilon q\Pr T_0\frac{dT_0}{dy} + ST_0 - \varepsilon ST_0^2 - \lambda ST_0^2 + \lambda\varepsilon ST_0^3 \\
 &- Ec\Pr\left(\frac{du_0}{dy}\right)^2 + \lambda Ec\Pr T_0\left(\frac{du_0}{dy}\right)^2 + \varepsilon Ec\Pr T_0\left(\frac{du_0}{dy}\right)^2 \\
 &- \lambda\varepsilon Ec\Pr T_0^2\left(\frac{du_0}{dy}\right)^2,
 \end{aligned} \tag{18}$$

$$\begin{aligned}
 p^2 : \frac{d^2u_2}{dy^2} &= \lambda T_0\frac{d^2u_1}{dy^2} + \lambda T_1\frac{d^2u_1}{dy^2} + q\frac{du_1}{dy} + \lambda\frac{du_0}{dy}\cdot\frac{dT_1}{dy} + \lambda\frac{du_1}{dy}\cdot\frac{dT_0}{dy} \\
 &- GrT_1 + 2\lambda GrT_0T_1,
 \end{aligned} \tag{19}$$

$$\begin{aligned}
 p^2 : \frac{d^2T_2}{dy^2} &= \varepsilon T_0\frac{d^2T_1}{dy^2} + \varepsilon T_1\frac{d^2T_0}{dy^2} + \lambda T_0\frac{d^2T_1}{dy^2} + \lambda T_1\frac{d^2T_0}{dy^2} - \lambda\varepsilon T_0^2\frac{d^2T_0}{dy^2} \\
 &- 2\lambda\varepsilon T_0T_1\frac{d^2T_0}{dy^2} + ST_1 + 2\varepsilon\frac{dT_0}{dy}\cdot\frac{dT_1}{dy} - 2\lambda\varepsilon T_0\frac{dT_0}{dy}\cdot\frac{dT_1}{dy} + \varepsilon q\Pr\frac{dT_1}{dy} \\
 &- \varepsilon q\Pr T_0\frac{dT_1}{dy} - \varepsilon q\Pr T_1\frac{dT_0}{dy} - 2\varepsilon ST_0T_1 - 2\lambda ST_0T_1 + 3\lambda\varepsilon ST_0^2T_1 \\
 &- 2Ec\Pr\frac{du_0}{dy}\cdot\frac{du_1}{dy} + 2\lambda Ec\Pr T_0\frac{du_0}{dy}\cdot\frac{du_1}{dy},
 \end{aligned} \tag{20}$$

⋮

The boundary conditions (7) are transformed also as

$$\begin{aligned}
 u_0(0) = 1, u_1(0) = u_2(0) = u_3(0) \dots = 0, \\
 u_0(1) = u_1(1) = u_2(1) = u_3(1) \dots = 0, \\
 T_0(0) = 1, T_1(0) = T_2(0) = T_3(0) \dots = 0, \\
 T_0(1) = T_1(1) = T_2(1) = T_3(1) \dots = 0.
 \end{aligned}
 \tag{21}$$

Since the zeroth order of the homotopy gives a linear ordinary differential equation, it is easily solvable without making recourse to initial guess. Therefore solving (15) and (16) and applying the boundary conditions $u_0(0) = 1$ and $u_0(1) = 0$, $T_0(0) = 1$ and $T_0(1) = 0$, we obtain the zeroth order solutions.

$$u_0 = A_1 y + A_2, \tag{22}$$

$$T_0 = B_1 y + B_2. \tag{23}$$

Solving (17) and (18) and applying the boundary conditions $u_1(0) = 0$ and $u_1(1) = 0$, $T_1(0) = 0$ and $T_1(1) = 0$, we obtain the solutions

$$u_1 = \frac{\lambda y^2}{2} - \frac{qy^2}{2} + \lambda Gr \left(\frac{y^2}{2} - \frac{y^3}{3} + \frac{y^4}{12} \right) - Gr \left(\frac{y^2}{2} - \frac{y^3}{6} \right) + A_3 y + A_4, \tag{24}$$

$$\begin{aligned}
 T_1 = & \frac{\varepsilon y^2}{2} - \frac{\lambda \varepsilon y^2}{2} + \frac{\lambda \varepsilon y^3}{6} - \frac{\varepsilon Pr y^2}{2} + \frac{\varepsilon q Pr y^2}{2} - \frac{\varepsilon q Pr y^3}{6} + S \left(\frac{y^2}{2} - \frac{y^3}{6} \right) \\
 & - \varepsilon S \left(\frac{y^2}{2} - \frac{y^3}{3} + \frac{y^4}{12} \right) - \lambda S \left(\frac{y^2}{2} - \frac{y^3}{3} + \frac{y^4}{12} \right) + \lambda \varepsilon S \left(\frac{y^2}{2} - \frac{y^3}{3} + \frac{y^4}{4} - \frac{y^5}{20} \right) \\
 & + \lambda Ec Pr \left(\frac{y^2}{2} - \frac{y^3}{2} \right) + \varepsilon Ec Pr \left(\frac{y^2}{2} - \frac{y^3}{2} \right) - \lambda \varepsilon Ec Pr \left(\frac{y^2}{2} - \frac{y^3}{3} + \frac{y^4}{12} \right) \\
 & - \frac{Ec Pr y^2}{2} + B_3 y + B_4,
 \end{aligned}
 \tag{25}$$

⋮

Equations (22) - (25) gives the approximation solutions for velocity and temperature as

$$u = u_{,0} + u_1 + u_2 + \dots \tag{26}$$

$$T = T_0 + T_1 + T_2 + \dots, \tag{27}$$

where,

$$\begin{aligned}
 A_1 = B_1 = -1, A_2 = B_2 = 1, \\
 A_3 = \frac{q}{2} + \frac{Gr}{3} - \frac{\lambda}{2} - \frac{\lambda Gr}{4}, \\
 B_3 = -\frac{q}{2} + \frac{\lambda \varepsilon}{3} - \frac{\varepsilon q Pr}{3} + \frac{q Pr}{2} + \frac{\varepsilon S}{4} + \frac{\lambda S}{4} - \frac{\lambda \varepsilon S}{5} - \frac{S}{3} + \frac{Ec Pr}{2} - \frac{\lambda Ec Pr}{3} \\
 - \frac{\varepsilon Ec Pr}{3} + \frac{\lambda \varepsilon Ec Pr}{4}, \\
 A_4 = B_4 = 0.
 \end{aligned}$$

To obtain the skin friction and rate of heat transfer at both plates, the expression for temperature and velocity are differentiated with respect to y , that is

$$\tau_0 = (1 - \lambda T) \frac{du}{dy} \Big|_{y=0} = -1 + A_3, \tag{28}$$

$$\tau_1 = (1 - \lambda T) \frac{du}{dy} \Big|_{y=1} = -1 + \lambda - q + \frac{\lambda Gr}{3} - \frac{Gr}{2} + A_3, \tag{29}$$

$$Nu_0 = (1 - \varepsilon T) \frac{dT}{dy} \Big|_{y=0} = -1 + B_3, \tag{30}$$

$$Nu_1 = (1 - \varepsilon T) \frac{dT}{dy} \Big|_{y=1} = -1 - \varepsilon - \frac{\lambda \varepsilon}{2} - q \text{Pr} + \frac{\varepsilon q \text{Pr}}{2} + \frac{S}{2} - \frac{\varepsilon S}{3} - \frac{\lambda S}{3} - \frac{\lambda \varepsilon S}{4} - Ec \text{Pr} + \frac{\lambda Ec \text{Pr}}{2} + \frac{\varepsilon Ec \text{Pr}}{2} - \frac{\lambda \varepsilon Ec \text{Pr}}{3} + B_3, \quad (31)$$

We further obtain the mass flux Q by evaluating the integral

$$Q = \int_0^1 u dy$$

$$Q = \frac{\lambda}{6} - \frac{q}{6} + \frac{\lambda Gr}{10} - \frac{Gr}{8} + \frac{A_3}{2}. \quad (32)$$

3 Results and Discussion

This problem considers a natural convection Couette flow between two vertical porous plates. The non-dimensional parameters governing the fluid flow are Grashof number, heat generation/absorption, Prandtl number, suction/injection, variable viscosity, thermal conductivity and the viscous dissipation. In this discussion, the value of Pr used is 0.71 which corresponds to the Prandtl number of air, q is chosen from -1.0 to 1.0 to account for suction as well as injection through the porous plates. The values of S are chosen between -1.0 and 1.0 to accommodate both heat generation and absorption. Similarly, the value of Gr is selected arbitrarily between 1 and 5 and $1 \leq Ec \leq 1.7$, $-1 \leq \lambda \leq 1$, $-1 \leq \varepsilon \leq 1$.

Figures 2 and 3 show the effect of Prandtl number on the fluid velocity and temperature. We notice that an increase in the Prandtl number Pr is to increase the temperature and velocity profiles. So the thickness of the thermal boundary layer decreases as Prandtl number increases. In heat transfer problems, the Prandtl number controlling the relative thickening of momentum and thermal boundary layers. The resultant effect of temperature increase is a corresponding strengthening of the convection current causing an increase in fluid velocity.

Figures 4 and 5 depict the effect of viscous dissipation on temperature and velocity profiles. It can be seen that the fluid velocity and temperature increase with the increase of viscous dissipation. More viscous dissipative heat causes rise in the velocity as well as temperature respectively. Consequently, the thermal boundary layer thickness is much pronounced in the presence of viscous dissipation.

The effect of Grashof number on the velocity and temperature profile is presented in figure 6 and 7. It is observed that the fluid velocity and temperature increase with the increase in Grashof number. This is physically expected, because the convection current grows. Consequently, the viscous dissipation heating is enhanced thereby causing an increase in the fluid temperature.

The influence of heat generation/absorption on the fluid velocity and temperature is shown in figures 8 and 9. It has been found that ($S < 0$) represents heat generation and ($S > 0$) represents heat absorption. It is clearly seen from the figures that as the heat generation ($S < 0$) increases, fluid temperature and velocity increase while it decreases with increase in heat absorption ($S > 0$). Increasing the heat generation parameter causes the fluid temperature to increase and it strengthens the convection current within the channel. In addition, increasing the heat absorption parameter causes a drop in fluid temperature and the thermal boundary layer becomes thinner thereby reduces the velocity distribution of the fluid as shown in figure 8.

To illustrate the effects of viscosity on the fluid temperature and velocity is presented in figures 10 and 11. It is observed that an increase in the fluid viscosity enhances the temperature and velocity profile. In addition, an increasing viscosity corresponds to the increasing resistance to flow which suppress the velocity of the working fluid, decreasing the viscosity contributes a decrease in the temperature of the working fluid.

Figures 12 and 13 display the effects for the velocity and temperature profiles for different values of variable thermal conductivity. It is clearly observed that velocity and temperature of the fluid increase as the thermal conductivity decreases. The thermal boundary layer thickness is also increased due to the corresponding strengthening of the convection currents caused by increase in the thermal conductivity and fluid velocity increases. However, an increase in the thermal conductivity of the fluid which causes an increase in the thermal boundary layer thickness resulting in temperature increase in the channel.

Figures 14 and 15 present the effects of suction/injection on the fluid velocity and temperature. It should be noted that ($q < 0$) signifies suction on the plate ($y=1$) with a corresponding injection ($q > 0$) on the ($y = 0$). It can be seen that as suction increases on the heated plate temperature within the channel responded with a decrease as shown in figure 15. This is physically expected since horizontal fluid motion is in the direction opposing the heat flux at ($y=1$), convection current is weak due to the decrease in temperature and as suction increases, velocity decreases through the heated plated.

Table 1 shows the skin friction on both plates. It is observed that an increase in viscosity and thermal conductivity have tendency to decrease the skin friction on both plates. Furthermore, injection contributes a decrease in the skin friction, and this due to velocity drop caused by increasing injection.

The rate of heat transfer on both walls is simulated and presented in table 2. From table 3, it is evident to show that injection leads to decrease in the heat transfer on the heated wall, and this due to temperature decrease caused by growing injection, which consequently leads to decrease in the rate of heat transfer on the heated wall. Moreover, Prandtl number Pr decreases rate of heat transfer on the heated wall, while it increases on the cold wall. This is due to the temperature increases with the increase in Pr leading to a decrease in the temperature gradient.

Table 3 presents the mass flux Q on both plates. It is clearly seen that the mass flux increases with the increase in injection and decreases with increasing suction. The table further shows that the mass flux decreases with increasing viscosity and conductivity.

4 Validation of results

By setting the viscous dissipation term, variable viscosity term, variable thermal conductivity term as well as suction/injection term to zero in the present problem, were cover the results of Jha and Ajibade (2010). The comparison is presented in table 4.

5 Conclusion

The present article has considered the effects of variable viscosity and thermal conductivity on steady natural convection Couette flow in the presence of suction/injection. The momentum and energy equations were solved using Homotopy perturbation method. The influence of the governing parameters on the velocity and temperature is presented graphically and discussed for varying values of the controlling parameters. The numerical values of skin friction, rate of heat transfer and mean temperature are presented in the tables. The work concluded that fluid velocity and temperature increase with an increase in Prandtl number. It is also observed that as suction increases on the heated plate temperature within the channel responded with a decrease. An increase in the thermal conductivity of the fluid which causes an increase in the thermal boundary layer thickness resulting in temperature increase in the channel. Finally, for the validity of our work, we have compared our results with the existing results of Jha and Ajibade (2010) shows that the present work agrees significantly.

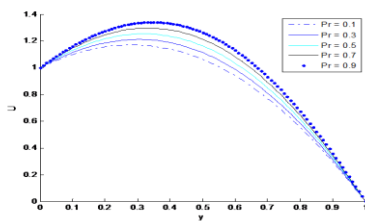


Fig 2: Velocity profile for different values of $Pr(Ec = 1.0, Gr = 7.0, S = 1.0, \lambda = -0.2, \varepsilon = -0.1, q = 1.0)$

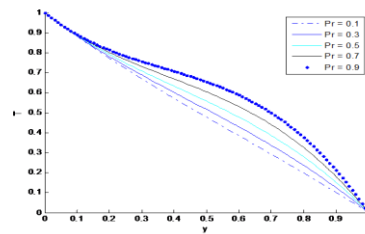


Fig 3: Temperature profile for different values $Pr(Ec = 1.0, Gr = 7.0, S = 1.0, \lambda = -0.2, \varepsilon = -0.1, q = 1.0)$

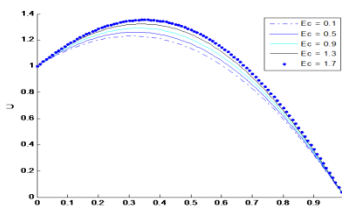


Fig 4: Velocity profile for different values of $Ec(Pr = 0.71, Gr = 7.0, S = 1.0, \lambda = -0.2, \varepsilon = -0.1, q = 1.0)$

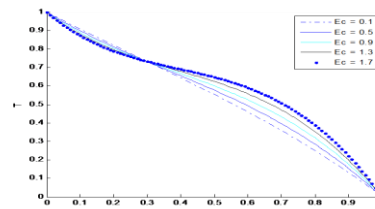


Fig 5: Temperature profile for different values $Ec(Pr = 0.71, Gr = 7.0, S = 1.0, \lambda = -0.2, \varepsilon = -0.1, q = 1.0)$

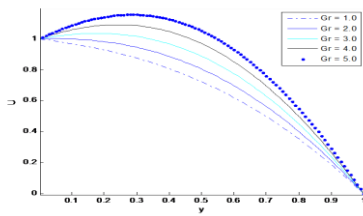


Fig 6: Velocity profile for different values of Gr ($Pr = 0.71, Ec = 1.0, S = 1.0, \lambda = -0.2, \varepsilon = -0.1, q = 1.0$)

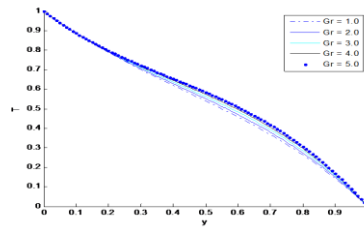


Fig 7: Temperature profile for different values Gr ($Pr = 0.71, Ec = 1.0, S = 1.0, \lambda = -0.2, \varepsilon = -0.1, q = 1.0$)

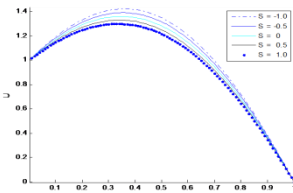


Fig 8: Velocity profile for different values of S ($Pr = 0.71, Ec = 1.0, Gr = 7.0, \lambda = -0.2, \varepsilon = -0.1, q = 1.0$)

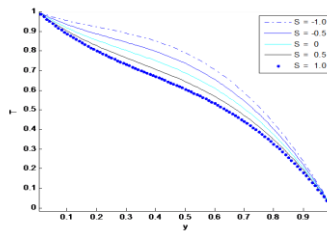


Fig 9: Temperature profile for different values S ($Pr = 0.71, Ec = 1.0, Gr = 7.0, \lambda = -0.2, \varepsilon = -0.1, q = 1.0$)

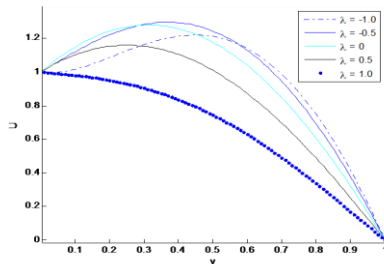


Fig 10: Velocity profile for different values of λ ($Pr = 0.71, Ec = 1.0, Gr = 7.0, S = -0.2, \varepsilon = -0.1, q = 1.0$)

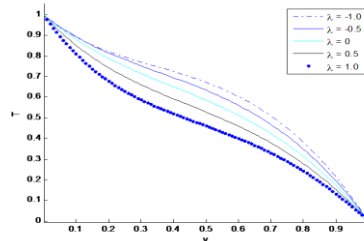


Fig 11: Temperature profile for different values λ ($Pr = 0.71, Ec = 1.0, Gr = 7.0, S = -0.2, \varepsilon = -0.1, q = 1.0$)

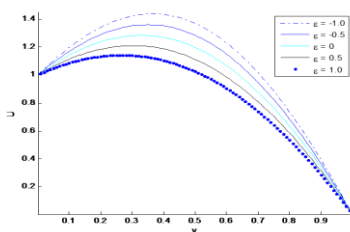


Fig 12: Velocity profile for different values of ε ($Pr = 0.71, Ec = 1.0, Gr = 7.0, S = -0.2, \lambda = -0.2, q = 1.0$)

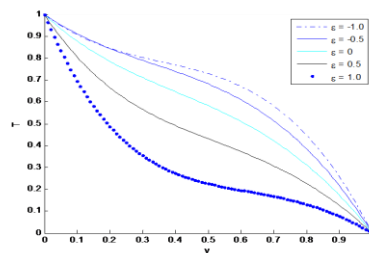


Fig 13: Temperature profile for different values ε ($Pr = 0.71, Ec = 1.0, Gr = 7.0, S = -0.2, \lambda = -0.2, q = 1.0$)

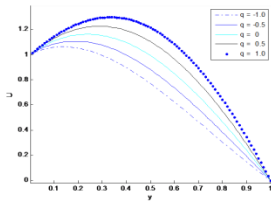


Fig 14: Velocity profile for different values of q ($Pr = 0.71, Ec = 1.0, Gr = 7.0, S = -0.2, \lambda = -0.2, \varepsilon = -0.1$)

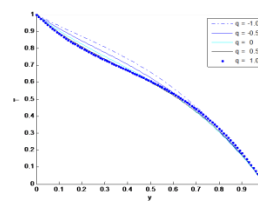


Fig 15: Temperature profile for different values of q ($Pr = 0.71, Ec = 1.0, Gr = 7.0, S = -0.2, \lambda = -0.2, \varepsilon = -0.1$)

Table 1: Estimated Numerical Values of Skin Friction τ_0 and τ_1

		$Ec = 0.7, Gr = 7.0, S = 1.0, \lambda = -0.4, \varepsilon = -0.2$		$Ec = 0.7, Gr = 7.0, S = 1.0, \lambda = -0.2, \varepsilon = -0.1$		
		q	τ_0	τ_1	τ_0	τ_1
Pr = 0.044	-1.0		1.73333	2.10000	1.28333	1.88333
	-0.5		1.98333	2.35000	1.53333	2.13333
	0.5		2.48333	2.85000	2.03333	2.63333
	1.0		2.73333	3.10000	2.28333	2.88333
Pr = 0.71	-1.0		1.69230	1.98102	1.12000	1.51000
	-0.5		1.71100	2.13621	1.56111	2.12220
	0.5		1.93880	2.31110	1.71333	2.30000
	1.0		2.16660	2.50000	2.01111	2.36666

Table 2: Estimated Numerical Values of Rate of Heat Transfer Nu_0 and Nu_1

		$Ec = 0.7, Gr = 7.0, S = 1.0, \lambda = -0.4, \varepsilon = -0.2$		$Ec = 0.7, Gr = 7.0, S = 1.0, \lambda = -0.2, \varepsilon = -0.1$		
		q	Nu_0	Nu_1	Nu_0	Nu_1
Pr = 0.044	-1.0		0.95563	0.21167	0.91050	0.21492
	-0.5		1.19389	0.47304	1.14876	0.47629
	0.5		1.67043	0.99577	1.62530	0.99902
	1.0		1.90869	1.25714	1.86357	1.26039
Pr = 0.71	-1.0		1.01716	0.44107	0.98365	0.38263
	-0.5		1.06599	0.49485	1.04432	0.56143
	0.5		1.16366	1.37351	1.16565	1.42826
	1.0		1.21249	1.81285	1.22632	1.86168

Table 3: Estimated Numerical Values of Mass Flux Q

		$Ec = 0.7, Gr = 7.0, S = 1.0, \lambda = -0.4, \varepsilon = -0.2$		$Ec = 0.7, Gr = 7.0, S = 1.0, \lambda = -0.2, \varepsilon = -0.1$		
		q	Q	Q		
Pr = 0.044	-1.0		0.31167	0.26000		
	-0.5		0.35333	0.30167		
	0.5		0.43667	0.38500		
	1.0		0.47833	0.42667		
Pr = 0.71	-1.0		0.43222	0.42222		
	-0.5		0.41000	0.40011		
	0.5		0.30111	0.29222		
	1.0		0.28333	0.26333		

Table 4: Comparison of Numerical Values between the Present Problem and Jha and Ajibade (2010)

S	Jha and Ajibade (2010)		Present Work	
	Velocity	Temperature	Velocity	Temperature
-1.0	0.98823	0.56975	0.98307	0.56901
-0.5	0.96151	0.53296	0.96029	0.53288
-0.5	0.91582	0.47030	0.91472	0.47038
1.0	0.89613	0.44340	0.89193	0.44410

References

- [1] Pop, H., and Watanabe, W. (1992). The effects of suction/injection in boundary layer flow and heat transfer on a continuous moving surface. *Technische Mechanik*. 13: 1-16
- [2] Shajaefard, M. H., Noorpoor, A. R., Avanesians, A., and Ghaffapour, M. (2005). Numerical investigation of flow control by suction and injection on a subsonic airfoil. *American Journal of Applied Sciences*. 20(10): 1474-1480.
- [3] Anuar, I., Roslinda, N. and Ioan, P.(2008). Uniform suction/blowing effect on flow and heat transfer due to stretching cylinder. *Applied Mathematical Modelling*. 32, 2059-2066.
- [4] Hazeem, A. A. (2010). The effect of suction and injection on unsteady Couette flow with variable properties. *Kragujevac Journal Science*. 32: 17-24.
- [5] Jha, B. K. and Ajibade, A. O. (2010). Unsteady free convective Couette flow of heat generating/absorbing fluid. *International Journal of Energy and Technology*. 2(12): 1-9.
- [6] Jha, B. K., Ajibade, A. O., and Andrew, O. (2011). Entropy generation under the effect of suction/injection. *Applied Mathematical Modelling*. 35(9), (2011), 4630-4646.
- [7] Bala, S. M., and Naikoti, K. (2011). Viscous dissipation effects on unsteady free convection and mass transfer flow past an accelerated vertical porous plate with suction. *Advances in Applied Science Research*. 2(6): 460-469.
- [8] Hazarika, G. C., and Uptal, S. G. (2012). Effects of variable viscosity and thermal conductivity on magnetohydrodynamics flow past a vertical channel. *Matematicas: Ensenanza Universitaria*. 10(2).
- [9] Daniel, S., Tella, Y., and Sani, U. (2013). An unsteady forced and free convection flow past an infinite permeable vertical plate. *International Journal of Science and Technology*. 3(3): 16-27.
- [10] Jha, B. K., Aina, B., and Sylvester, B. J.(2013). Natural convection flow in a vertical micro-channel with suction/injection. *Proceeding of the Institution of Mechanical Engineers, Part E: Journal of Process Mechanical Engineering*. 228:171. Doi: 10.1177/0954408913492719.
- [11] Borah, G., and Hazarika, G. C. (2013). Effects of variable viscosity and thermal conductivity and magnetic field effect on the free convection and mass transfer flow through porous medium with constant suction/heat flux. *Journal of Computer and Mathematical Sciences*. 4(6): 407-418.
- [12] Oahimire, J. I., and Olajuwon, B. I. (2013). Hydromagnetic flow near a stagnation point on stretching sheet with variable thermal conductivity and heat generation. *International Journal of Applied Science and Engineering*. 11(3): 331- 341.
- [13] Uwanta, I. J., and Hamza, M. M. (2014). Effect of suction/injection on unsteady hydromagnetic Convective flow or reactive viscous fluid between vertical porous plates with thermal diffusion. *International Scholarly Research Notices*. ID: 980270, 14.
- [14] Jha, B. K, Aina, B., and Ajiya, A. T. (2015). Role of suction/injection on magnetohydrodynamics natural convection flow in a vertical micro-channel. *International Journal of Energy and Technology*. 2(10): 1-7.
- [15] Jha, B. K., Chiboke, I., and Sylvester, B. J. (2015). Effects of suction/injection-combination on transient free convective-radiative flow in a vertical porous channel. *Proceeding of the Institution of Mechanical Engineers, Part E: Journal of Process Mechanical Engineering*. 1989:1996.
- [16] Santana, H., and Hazarika, G. C. (2015). Effects of variable viscosity and thermal conductivity on magnetohydrodynamics free convection and mass transfer flow over an inclined vertical surface in a porous medium with heat generation. *International Journal of Engineering Sciences*. 4(8): 20-27.

- [17] Omokhuale, E., and Ovwasa, M. O. (2016). The effect of heat source on free convection Fluidflow in a vertical channel with chemical reaction. *International Journal of Science for Global Sustainability*. 2(4): 2488-9229.
- [18] Hazarika, G. C., and Phukan, B. (2017). Effects of variable viscosity and thermal conductivity on steady magnetohydrodynamics flow of a micropolar fluid through a specially characterize ed horizontal channel. *AMSE Journals-AMSE IIETA Puublication-2017-series*. 86(1): 1-13.
- [19] Tafida, M. K., and Ajibade, A. O. (2019). Studied the effect of variable viscosity on natural convection flow between vertical parallel plates in the presence of heat generation/absorption. *Asian Research Journal of Mathematics*. 14(3): 1-15
- [20] Ajibade, A. O., and M. K. Tafida. (2020). The combined effect of variable viscosity and variable thermal conductivity on natural convection Couette flow. *International Journal of Thermofluids*. 5-6: 100036.
- [21] He, J. H. (1999). Homotopy Perturbation Methods Technique. *Computer Method in Applied Mechanics and Engineering*. 178: 257-262
- [22] Dau-Hua S. (2009). Homotopy perturbation method for nonlinear oscillators. *Computers and Mathematics with Applications*. 58:2456-2459.
- [23] Abou-Zeid, M. (2017). Homotopy perturbation method for magnetohydrodynamics non-Newtonian nanofluid flow through a porous medium in eccentric annuli with peristalsis. *Thermal Science*. 21: 2058 – 2069.
- [24] Sara, A. I., and Bhatti, M. M. (2018). The impact of impinging TiO₂ nanoparticles in Prandtl nanofluid along with endoscopic and variable magnetic field effects on peristaltic Bloodflow. *Multidiscipline Modeling in Materials and Structures*. 14(3): 530-548.